

Photo-Induced Evolution of Randomly Rough Surfaces of Amorphous Chalcogenide Films

Yuri Kaganovskii,* Valentin Freilikher, and Michael Rosenbluh

Photoinduced (PI) evolution of statistically rough surfaces of amorphous chalcogenide films $\text{As}_{20}\text{Se}_{80}$ at room temperature has been studied by measuring the angular dependence of the intensity of light scattered from a surface illuminated by CW laser ($\lambda = 660$ nm). The interpretation of the scattering data based on the resonant scattering theory enables to confirm unequivocally the diffusion mechanism of PI mass transfer. It is detected that the change of the amplitude of a spatial harmonic in the roughness spectra strongly depends on its period Λ . During illumination, the amplitude increases at $\Lambda > \Lambda^*$, whereas harmonics with $\Lambda < \Lambda^*$ decreases by Λ^* , which corresponds to zero evolution rate, is found to be $6.7 \mu\text{m}$. In accordance with our theoretical prediction, both growth and decrease are exponential with the rates depending on Λ . As the result, the roughness with initial rms height of $50\text{--}70$ nm transforms into quasiperiodic surface grating with the average amplitude of about 400 nm and average period close to $15 \mu\text{m}$. From the kinetics of time variation of the scattered intensity, the PI diffusion coefficient D is calculated. When the laser intensity changes from 5.6 to 14 W cm^{-2} , D is found in the range 1×10^{-13} – $3.4 \times 10^{-13} \text{ m}^2 \text{ s}^{-1}$.

1. Introduction

Amorphous chalcogenide films (ACFs) are of great interest for optics and microelectronics due to their unusual optical properties and high photo sensitivity. Under the influence of laser illumination, ACFs change their refractive index, transparency, mechanical and electric properties, and surface profile. Photo-induced (PI) mass transfer is a subject of multiple studies; however, the physics of this phenomenon is not yet clearly understood and still discussed in the literature.^[1] During the years passed since the discovery of PI mass transfer in ACFs,^[2] its mechanism was believed to be the viscous flow caused by the

electric field gradient of the incident light,^[3–6] which lowers the film viscosity.

In contrast to above-mentioned mechanism of viscous flow and optical driving force, we suggest that PI mass transfer occurs by atomic diffusion motion of chalcogens and pnictides.^[7] The Stokes–Einstein relation, which for many materials links diffusion and viscosity coefficients, fails for ACFs,^[8] and thus the diffusion is an independent mechanism of mass transfer.

Two main driving forces of PI diffusion have been considered. The first one is the lateral steady state electric field E . Under illumination by light with photon energy close to the bandgap of the ACF material (band gap illumination), non-equilibrium carriers, electrons, and holes, are generated, their concentration being proportional to the absorbed light energy. If there is a density gradient of carriers, they diffuse along the film in the direction opposite to the gradient.

Due to the difference in the mobilities of electrons and holes, a lateral electric field arises in the film (Dember field^[9]). If the film contains irregularities, either periodic, or random, the lateral field arises not only under the intensity gradient of the incident light, but also under uniform illumination. Previously it was shown^[7,10] that for a sinusoidal surface profile, $z(x) = h \sin qx$, a lateral electric field E with the period $\Lambda = 2\pi/q$ was due to the illumination by uniform light. This field determines the electric driving force, f_E , for the diffusion flux


$$f_E(x) = q_{\text{eff}} E(x) \quad (1)$$

Effective electric charge, q_{eff} , of ACF constituents appears due to the motion of the electrons and holes in electric field that creates so-called electronic and hole winds.^[11] Atoms are dragged by electrons and holes moving in an electric field, so that the resulting value and sign of q_{eff} depends on the cross-section of scattering of the carriers on the atoms. It was previously shown^[12] that the mass transfer in $\text{As}_{20}\text{Se}_{80}$ films was directed towards higher light intensity where surface profile had a positive curvature. Thus, the electric force stimulates growth of the grating amplitude. The second force f_L , is caused by capillary pressure (Laplace pressure), which appears due to the surface roughness. In the case of the periodic surface,^[13] f_L equals to

$$f_L = q^2 \gamma \times \Omega \times h \times \sin qx [1 - \exp(-qH_0)] \quad (2)$$

herein, γ is the surface tension, H_0 is the average thickness of the film, Ω is the average atomic volume. The Laplace pressure

Y. Kaganovskii, V. Freilikher, M. Rosenbluh
 Department of Physics
 Bar-Ilan University
 Ramat-Ran 52900, Israel
 E-mail: kagany@biu.ac.il

 The ORCID identification number(s) for the author(s) of this article can be found under <https://doi.org/10.1002/pssa.202300546>.

© 2023 The Authors. physica status solidi (a) applications and materials science published by Wiley-VCH GmbH. This is an open access article under the terms of the Creative Commons Attribution-NonCommercial License, which permits use, distribution and reproduction in any medium, provided the original work is properly cited and is not used for commercial purposes.

DOI: 10.1002/pssa.202300546

flattens the surface profile, i.e., the capillary force opposes the electrical force. Since f_L and f_E depend differently on the period Λ , the evolution of the surface profile also depends on Λ , so that the amplitude, h , of the grating varies with the time of illumination following the exponential law^[7]

$$h(t) = h_0 \exp(-\kappa \times t) \quad (3)$$

where h_0 is the amplitude at $t = 0$

$$\kappa = -\frac{Bq^2}{(1 + q^2 l^2)} + Aq^3 \quad (4)$$

$$B = \frac{D}{kT} q_{\text{eff}} \varphi_0; \quad A = \frac{D}{kT} \Omega \gamma (1 - e^{-qH_0}) \quad (5)$$

$D = D_p c + D_C (1 - c)$ is the effective diffusion coefficient, D_p and D_C being diffusion coefficients of pnictides and chalcogens, respectively, and c is the concentration of pnictide atoms,^[14,15] k is the Boltzmann constant, T is absolute temperature. As described previously, the driving forces compete with one another and due to competition between f_L and f_E , the constant k changes its sign at some period Λ^* : k is positive when profile flattens and negative when the grating amplitude increases. Measuring the flattening constant k for given Λ , one can determine the PI diffusion coefficient D .^[7]

In the present article, we study the PI mass transfer of randomly rough surfaces of amorphous chalcogenide films and show, both experimentally and theoretically, that the main mechanism of PI mass transfer is the atomic diffusion motion of chalcogens and pnictides, rather than the viscosity change. We used the light scattering method, which enabled retrieving the spatial power spectrum of an arbitrary surface profile from the angular dependence of the back-scattered intensity. The algorithm of the retrieval is based on the fact that the scattering from a small (compare to the wavelength λ) roughness is of a resonant nature: intensity scattered in a given direction θ_s is proportional to the amplitude of the spatial harmonic with the period $\Lambda = \lambda / \sin \theta_s$. It is shown that the kinetics of PI mass transfer significantly depends on the profile of the surface, i.e., on its power spectrum. Under illumination, the amplitudes exponentially increase at $\Lambda > \Lambda^*$, whereas those of harmonics with $\Lambda < \Lambda^*$ exponentially decrease. The boundary value Λ^* corresponds to the harmonic with zero evolution rate, for which the electrical and capillary forces are equal. In our experiments, $\Lambda^* \approx 6.7 \mu\text{m}$ and the maximum rate of growth corresponded to $\Lambda \approx 15 \mu\text{m}$, in agreement with the theoretical estimates. The experiments and theoretical results unequivocally confirm the diffusive mechanism of PI mass transfer.

We also demonstrate coarsening of surface roughness under light illumination and transformation of random roughness into quasi-periodic PI ripples observed on the surface of ACFs.^[10,16,17]

2. Variation of Scattering Intensity in the Process of Roughness Evolution

Let us consider light scattering by a “one-dimensional” rough surface, the shape of which is given by a random function $z(x, t)$. If the roughness is smooth enough ($|\frac{\partial z}{\partial x}| \ll 1$) and its

root-mean-square (rms) height σ is small as compared to the wavelength of light λ ($\sigma \ll \lambda$), the scattering properties of such a surface are defined by its correlation function $W(x_1, x_2) = \langle z(x_1) \cdot z(x_2) \rangle$; $\langle \dots \rangle$ indicates statistical averaging over the ensemble of $z(x)$ realizations. If the roughness is statistically uniform (this is quite well satisfied in our case), then W depends only on the difference $\rho = x_1 - x_2$.

The theory of wave diffraction on such a surface^[18] gives the following formula for the intensity of light scattered in the direction of angle θ_s to the z -axis (far zone)

$$I(\theta_s) = \frac{4q^4 S}{R_1^2 R_2^2} Q(\theta_s, \theta_{\text{in}}) \times \tilde{W}(q) \quad (6)$$

where S is the area of the illuminated region, R_1 and R_2 are the distances from surface to source and receiver respectively (Source and receiver were in a zone a long way from the specimen, so the distances R_1 and R_2 could be introduced), $Q(\theta_s, \theta_{\text{in}})$ is a smooth [as compared to $W(q)$] function of the angles of scattering θ_s and incidence θ_{in} , which depends on the optical constants of the sample and on the polarization of light, $q = \frac{2\pi}{\lambda} (\sin \theta_s - \sin \theta_{\text{in}})$; $\tilde{W}(q)$ is the Fourier transform of the correlation function

$$\tilde{W}(q, t) = \frac{1}{2\pi} \int W(\rho, t) \times e^{-iq\rho} d\rho \quad (7)$$

This function presents the spatial spectrum of the rough surface.

Equation (6) presents the so-called resonant scattering mechanism, the physical meaning of which is rather clear: the intensity of the field scattered at the angle $\theta_s - \theta_{\text{in}}$ is proportional to the Fourier transform of the correlation function with argument q , which means that only the harmonic with $\Lambda = 2\pi/q$ participates in light scattering in this direction. Formula (6) also shows that the time variation in the intensity of scattered light $I(\theta_s, t)$ is governed by the time dependence of $\tilde{W}(q, t)$.

Taking into account Equation (3) we obtain the following expression for the time evolution of a sinusoidal harmonic

$$z(x, t) = \int \tilde{z}(q, 0) \exp[iqx - \kappa(q) \times t] dq \quad (8)$$

Then, the correlation function of the surface can be presented as

$$W(\rho, t) = \iint \langle \tilde{z}(q_1, 0) \tilde{z}^*(q_2, 0) \rangle \exp\{iq_1 x_1 - iq_2 x_2 - [\kappa(q_1) + \kappa(q_2)] \times t\} dq_1 dq_2 \quad (9)$$

Since the function W depends on the difference of $x_1 - x_2$, the following equality is satisfied^[18]

$$\langle \tilde{z}(q_1, 0) \tilde{z}^*(q_2, 0) \rangle = \delta(q_1 - q_2) \tilde{W}(q_1, 0) \quad (10)$$

Substituting (10) into (9) we get

$$W(\rho, t) = \int \tilde{W}(q, t) \exp[iq\rho - 2\kappa(q)t] dq \quad (11)$$

Comparison of Equation (7) and (11) gives the following time dependence of the Fourier transform of the correlation function

$$\tilde{W}(q, t) = \tilde{W}(q, 0) \exp[-2\kappa(q)t] \quad (12)$$

After substitution of Equation (12) into (6) we obtain

$$I(q, t) = I(q, 0) \exp[-2\kappa(q)t] \quad (13)$$

where the exponent $\kappa(q)$ is determined by the constants characterizing the PI mass transfer kinetics in accordance with Equations (4) and (5). It is evident from Equation (13) that the intensity of light scattered at the angle $\theta_s - \theta_{in}$ (i.e., for given q) varies exponentially with time and, depending on the sign of k , either increases or decreases as the surface relief grows or flattens. As the time behavior of the scattering intensity at different angles is measured, we can obtain the function $k(q)$ and then determine the PI diffusion coefficient D from Equation (3)–(5).

3. Experimental Section

We have investigated the kinetics of the PI variation of a statistically rough surface of $\text{As}_{20}\text{Se}_{80}$ films at room temperature. As it was previously shown,^[17] PI mass transfer in the films of such composition occurs much faster compared to stoichiometric and other As-Se compositions. Typical transmission spectrum of the film is shown in **Figure 1**.

PI evolution of the roughness was studied under illumination by a polarized diode laser ($\lambda = 660$ nm) with various incident powers P_0 from 10 to 25 mW. The photon energy of the laser used for illumination (≈ 1.88 eV) was near the band gap of the film material ($E_g \approx 1.83$ eV), calculated from the spectrum in **Figure 1**.

The rough surfaces of the films $\text{As}_{20}\text{Se}_{80}$ were prepared in two steps. First, we produced a random, “one-dimensional” (depending on a single coordinate) micro-relief on a glass substrate by rubbing it against finely dispersed sandpaper. The micro-roughness on the glass substrates was analyzed by atomic force microscopy (AFM). At the second step, $\text{As}_{20}\text{Se}_{80}$ films with the thickness about 2 μm were thermally deposited on the rough surface in 10^{-5} Torr vacuum. The surface of the films reproduced roughness of the substrates, and initial rms varied from 50 to 70 nm. Since the film thickness noticeably exceeded the rms

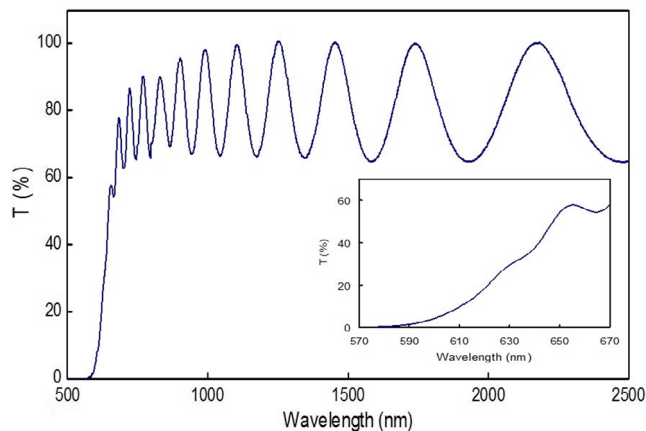


Figure 1. Transmission spectrum of $\text{As}_{20}\text{Se}_{80}$ film of 2 μm thick. Inset shows a part of spectrum near the band gap edge.

of the roughness on the glass substrate, the driving forces of PI mass transfer in the chalcogenide films did not change due to substrate roughness.

The polarization direction was normal to the direction of scratches on the surface because the kinetics of the mass transfer in the direction parallel to the polarization vector is a few times faster than in the perpendicular direction.^[13] The surface area illuminated by the laser beam had an elliptic shape with a and b hemi axes equal ≈ 365 and $124 \mu\text{m}$, respectively, and thus the incident laser intensity $I_0 = P_0(1 - R)/\pi ab$ varied from 5.6 to 14 W cm^{-2} with the film reflectivity R about 18%. During illumination, after different times, we measured the angular distribution of light scattered by the film surface. The angle of incidence was 4.5° ; the intensity of the scattered light was measured with a detector scanned in the horizontal plane in a circular pattern with the center of the scan located on the sample. To improve the signal-to-noise ratio the laser was chopped at about 210 Hz and a lock-in amplifier was used. The accuracy of the scattering angle measurements was 0.01.

4. Results

Shown in **Figure 2** are the angular distributions of the scattered intensity, $I(\theta_s)$, measured at different times during illumination. As it is seen, at angles smaller than 11° – 12° , the scattered intensity grows with the illumination time, whereas at larger angles the intensity decreases (see inset).

As it was indicated above, the scattered intensity at the angle $\theta_s - \theta_{in}$ is proportional to the amplitude $\tilde{W}(q)$ of the periodic component of the Fourier-expansion of the random profile $z(x)$ with the period $\Lambda = 2\pi/q = \lambda/(\sin\theta_s - \sin\theta_{in})$. It means that for $\lambda = 660$ nm and $\theta_{in} = 4.5^\circ$, the scattering at angles from 6° to 20° corresponds to the periodic harmonics with Λ from 25 to $2.4 \mu\text{m}$. In particular, the angle 11° , where we observe switching of the scattered intensity from grows to decrease, corresponds to $\Lambda^* = 6.7 \mu\text{m}$.

In **Figure 3**, one can see the growth of the scattered intensity with time of illumination for harmonics with $\Lambda > \Lambda^*$ and its decrease for $\Lambda < \Lambda^*$. Considering Equation (13), we present

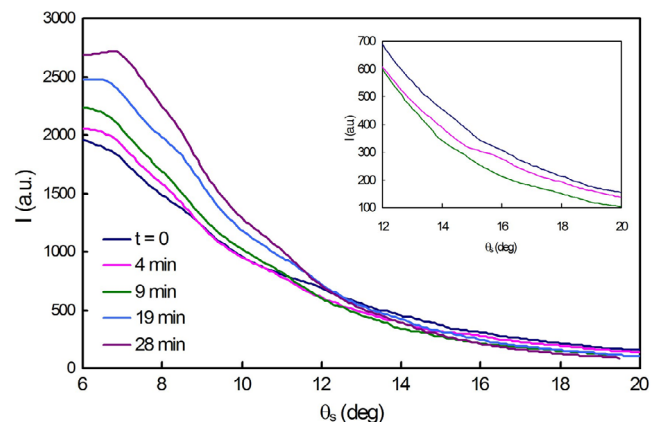


Figure 2. Dependence of the scattered intensity on the scattering angle at various times of illumination. Incident laser power $P = 25$ mW. The inset shows the decrease of the scattered intensity at $12 < \theta_s < 20^\circ$.

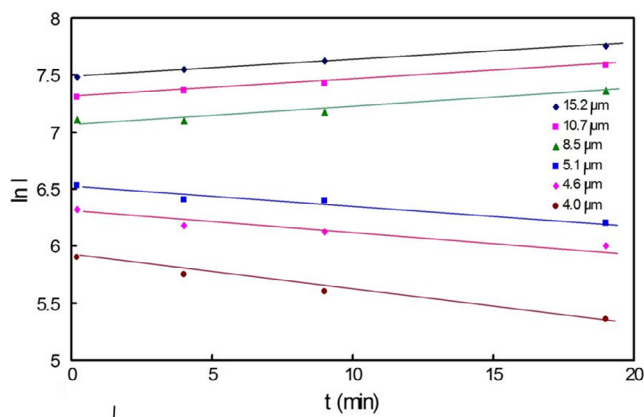


Figure 3. Plots $\ln I$ vs t for different harmonics of the roughness spectra. The scattered intensity grows for harmonics with $\lambda > \lambda^*$ and decreased for harmonics with $\lambda < \lambda^*$, $P = 25$ mW. The periods λ are calculated for angles of scattering 7° – 9° and 12° – 14° using formula $\lambda = \lambda / (\sin \theta_s - \sin \theta_{in})$.

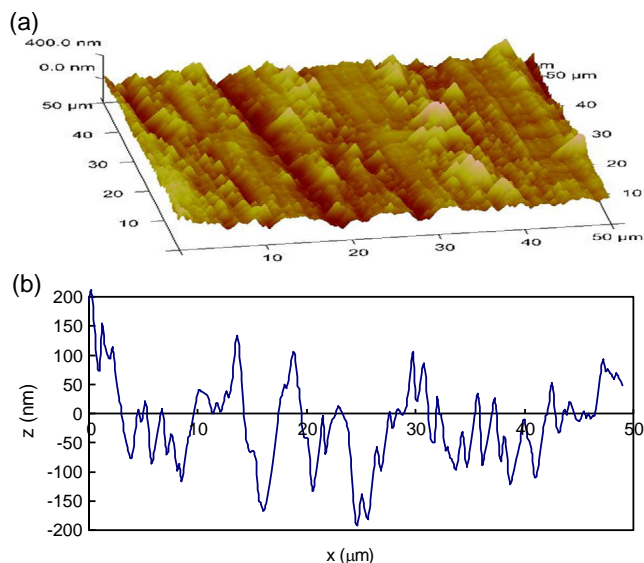


Figure 4. a) AFM image of the film surface before illumination; b) the cross-section in the direction normal to the scratches.

the intensity variation in the coordinates $\ln I$ vs t . The slopes of the straight lines in Figure 3 are equal to $2k$. Positive slope describes growth of amplitude for harmonics with $\lambda > \lambda^*$, whereas the negative slope corresponds to the amplitude smoothing for harmonics with $\lambda < \lambda^*$.

The AFM measurements of the surface roughness have been carried out before (Figure 4) and after (Figure 5 and 6) illumination for various times.

Figure 5b and 6b clearly demonstrate coarsening of the roughness due to illumination: the amplitude of harmonics with large λ grows, as well as the rms height of the roughness, whereas harmonics with small λ are smoothed, in accordance with the theoretical prediction above. In Figure 7, two Fourier transform (FT) plots are presented, which correspond to profiles shown in

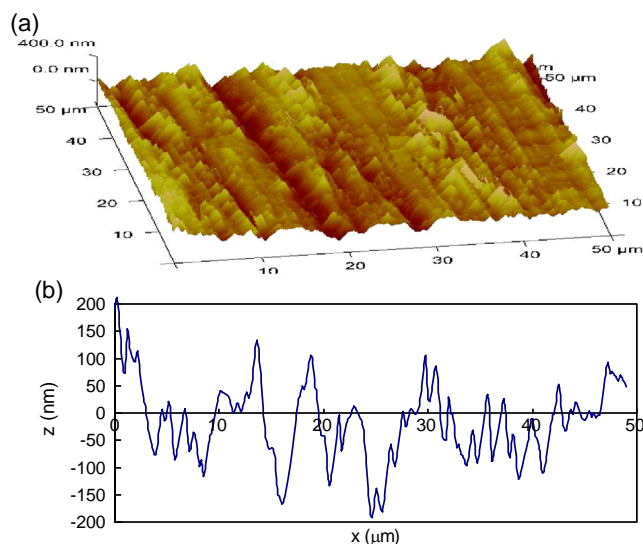


Figure 5. a) AFM image and b) the profile of the film surface after illumination during 20 min with the beam intensity 14 W cm^{-2} .

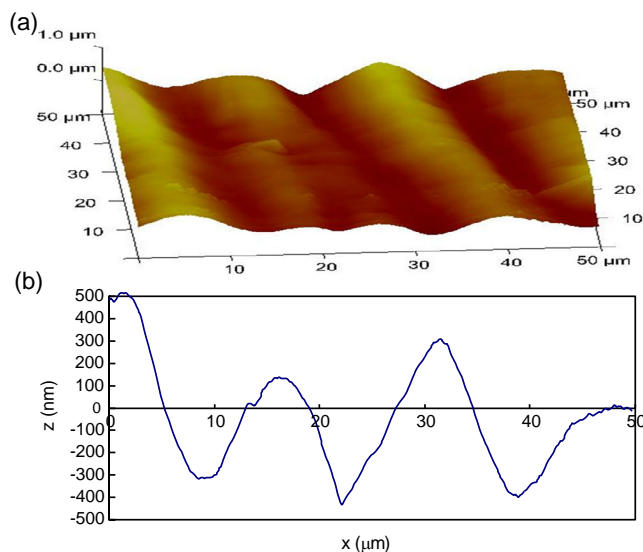


Figure 6. a) AFM image and b) the profile of the film surface after illumination during 76 min with the beam intensity 14 W cm^{-2} .

Figure 5b and 6b, respectively. As it is seen, amplitudes of harmonics with $q > 0.15 \mu\text{m}^{-1}$ ($\lambda < 6.7 \mu\text{m}$) decrease with time, whereas the amplitudes of harmonics $q < 0.15 \mu\text{m}^{-1}$ grow, in accordance with the variation of scattered intensity (Figure 2 and 3)

Due to coarsening, after long enough time of illumination the surface becomes almost periodic with average amplitude and period of about 400 nm and $15 \mu\text{m}$ respectively. As predicted,^[10] this period corresponds to harmonic whose amplitude grows with the maximum rate. Indeed, as it is seen in Figure 2, the maximum of the scattered intensity is observed at $\theta_s \approx 7^\circ$, which corresponds to $\lambda = 15.2 \mu\text{m}$.

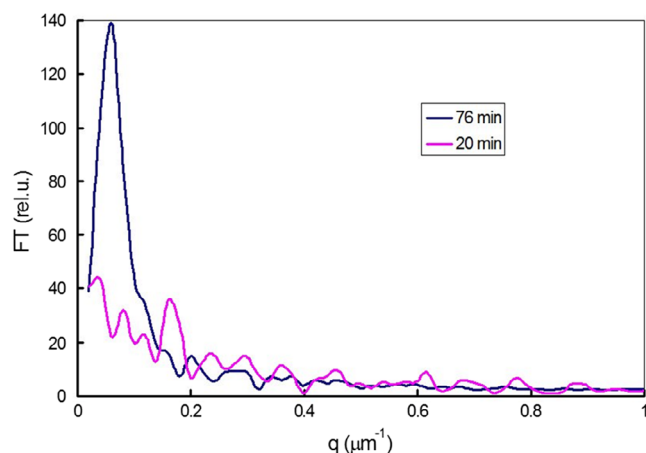


Figure 7. Fourier transform of profiles presented in Figure 4b and 5b, respectively. The wave numbers $0.15 < q < 1 \mu\text{m}^{-1}$ correspond to $6.7 > \Lambda > 1 \mu\text{m}$. Maximum in the plot (for 76 min) corresponds to $\Lambda \approx 15 \mu\text{m}$.

PI diffusion coefficients, D , calculated from the slopes of the straight lines in Figure 3 using Equation (4) and (5), varied in a range 1×10^{-13} – $3.8 \times 10^{-13} \text{ m}^2 \text{ s}^{-1}$ with the laser intensity changed from 5.6 to 14 W cm^{-2} . These results agree with the previous measurements of D (see refs. [8,13]).

5. Discussion

The results of our experiments are in agreement with the predictions of diffusion mechanism of PI mass transfer, in contrast previously proposed viscous flow. Since we observed the evolution of surface roughness under uniform illumination, the gradient of electric field of light cannot be considered as a driving force of PI mass transfer. In contrast, we demonstrated a competition between the electric and capillary driving forces that completely confirmed our model of PI mass transfer. The “boundary” period $\Lambda^* \approx 6.7 \mu\text{m}$, at which the evolution of Fourier harmonics under uniform laser illumination switched from grows to smoothing, is close to the previously reported^[7] value $8 \mu\text{m}$, obtained for sinusoidal profiles on the same material. Possible explanation of the difference is that Λ^* depends on the light intensity, which in ref. [7] was lower than in our experiments with the surface roughness.

Atomic redistribution caused by breaking of bonds under band gap illumination,^[3] stimulates atomic diffusion independent of viscosity. The viscous flow in ACFs occurs by sliding of structural elements (chains and rings) relatively to one another, which is facilitated by defects in intermolecular bonds. The atomic diffusion, i.e., individual atomic jumps, is caused by intramolecular reconstruction and thus not directly related to the viscous flow. This difference explains why the relationship between D and η for amorphous chalcogenides does not follow to Stokes–Einstein relation.

One of results of this article, important for applications, consists in the coarsening and development of the roughness under band gap illumination. This concerns a micro-roughness, with rms σ of the order of nanometers. As it follows from our analysis

and previous observations,^[10,17,18] even such small roughness would be transformed into harmonics with the period 12 – $15 \mu\text{m}$ and amplitude in tens nanometers.

6. Conclusion

Evolution of statistically rough surface of amorphous chalcogenide films $\text{As}_{20}\text{Se}_{80}$ under band gap illumination at room temperature was measured using methods of light scattering and AFM and explained in frames of our theory of PI mass transfer that completely confirms the diffusion theory. It is detected that the amplitude of harmonics in the roughness spectra with the periods $\Lambda > 6.7 \mu\text{m}$ increases during illumination, whereas harmonics with $\Lambda < 6.7 \mu\text{m}$ decrease, in accordance with our theoretical predictions. Both growth and decrease of the amplitude of harmonics are exponential and the rate depends on Λ . Maximum rate of growth corresponds to $\Lambda \approx 15 \mu\text{m}$, and the micro-roughness transforms under uniform band gap illumination into quasi-periodic surface profile with period close to $15 \mu\text{m}$ and average amplitude noticeably exceeding initial rms of the roughness. PI diffusion coefficients, D , calculated from the kinetics of growth and smoothing amplitude of harmonics in the roughness spectrum agree with previous results.

Conflict of Interest

The authors declare no conflict of interest.

Data Availability Statement

The data that support the findings of this study are available from the corresponding author upon reasonable request.

Keywords

amorphous chalcogenide films, diffusion, photo-induced mass transfer, resonant light scattering, surface roughness

Received: July 24, 2023

Revised: November 28, 2023

Published online: January 1, 2024

- [1] K. Tanaka, *J. Non-Cryst. Solids* **2018**, 500, 272.
- [2] K. E. Asatryan, T. Galstian, R. Valle'e, *Phys. Rev. Lett.* **2005**, 94, 087401
- [3] H. Fritzsche, *Phys. Rev. B* **1995**, 52, 15854.
- [4] J. Kumar, L. Li, X. Li Jiang, D.-Y. Kim, T. Seung Lee, S. Tripathy, *Appl. Phys. Lett.* **1998**, 72, 2096.
- [5] V. K. Tikhomirov, *J. Non-Cryst. Solids* **1999**, 256 & 257, 328.
- [6] V. K. Tikhomirov, K. Asatryan, T. V. Galstian, R. Vallee, A. B. Seddon, *Philos. Mag. Lett.* **2003**, 83, 117.
- [7] Yu. Kaganovskii, V. Freilikher, M. Rosenbluh, *J. Non-Cryst. Solids* **2022**, 588, 121611.
- [8] Yu. Kaganovskii, D. L. Beke, V. Freilikher, S. Kökényesi, A. M. Korsunsky, *Mater. Res. Express* **2020**, 7, 016204.
- [9] H. Dember, *Phys. Z.* **1931**, 32, 856.
- [10] Yu. Kaganovskii, A. M. Korsunsky, M. Rosenbluh, *Mater. Lett.* **2016**, 183, 156.

- [11] V. B. Fiks, in *Ion Conductivity in Metals and Semiconductors (Electrotransport)*, Nauka, Moscow **1969**.
- [12] M. L. Trunov, P. M. Lytvyn, *J. Non-Cryst. Solids* **2018**, 493, 86.
- [13] Yu. Kaganovskii, M. L. Trunov, D. L. Beke, S. Kökényesi, *Mater. Lett.* **2012**, 66, 159.
- [14] Yu. Kaganovskii, D. L. Beke, S. Kökényesi, *Appl. Phys. Lett.* **2010**, 97, 061906.
- [15] Yu. Kaganovskii, D. L. Beke, S. Charnovych, S. Kökényesi, M. L. Trunov, *J. Appl. Phys.* **2011**, 110, 063502.
- [16] M. L. Trunov, P. M. Nagy, V. Takats, P. M. Lytvyn, S. Kökényesi, E. Kalman, *J. Non-Cryst. Solids* **2009**, 355, 1993.
- [17] K. Tanaka, M. Mikami, *J. Non-Cryst. Solids* **2012**, 358, 2385.
- [18] F. G. Bass, I. M. Fuks, in *Scattering of Waves by a Statistically Rough Surface*, Nauka, Moscow **1972**.